Geophysical Research Letters

RESEARCH LETTER
10.1029/2020GL088865

Proglacial Lakes Control Glacier Geometry and Behavior During Recession

J. L. Sutherland[1], J. L. Carrivick[1], N. Gandy[2], J. Shulmeister[3], D. J. Quincey[1], and S. L. Cornford[4]

[1]School of Geography and water@leeds, University of Leeds, Leeds, UK, [2]School of Earth and Environment, University of Leeds, Leeds, UK, [3]School of Earth and Environment, University of Canterbury, Christchurch, New Zealand, [4]Department of Geography, Swansea University, Swansea, UK

Key Points:
- A reverse bedslope, combined with deep water and frontal ablation, produces a terminus geometry with a wider and steeper ice surface slope
- A lake-terminating glacier receded >4 times further and flowed up to 8 times faster than a land-terminating glacier forced by the same climate
- Our simulated lake processes predominantly influenced the glacier over decades to centuries rather than over millennia

Supporting Information:
- Supporting Information S1

Correspondence to:
J. L. Sutherland,
gyjls@leeds.ac.uk

Citation:
Sutherland, J. L., Carrivick, J. L., Gandy, N., Shulmeister, J., Quincey, D. J., & Cornford, S. L. (2020). Proglacial lakes control glacier geometry and behavior during recession. *Geophysical Research Letters*, *47*, e2020GL088865. https://doi.org/10.1029/2020GL088865

Received 21 MAY 2020
Accepted 8 SEP 2020
Accepted article online 21 SEP 2020

Abstract Ice-contact proglacial lakes are generally absent from numerical model simulations of glacier evolution, and their effects on ice dynamics and on rates of deglaciation remain poorly quantified. Using the BISICLES ice flow model, we analyzed the effects of an ice-contact lake on the Pukaki Glacier, New Zealand, during recession from the Last Glacial Maximum. The ice-contact lake produced a maximum effect on grounding line recession >4 times further and on ice velocities up to 8 times faster, compared to simulations of a land-terminating glacier forced by the same climate. The lake contributed up to 82% of cumulative grounding line recession and 87% of ice velocity during the first 300 years of the simulations, but those values decreased to just 6% and 37%, respectively, after 5,000 years. Numerical models that ignore lake interactions will, therefore, misrepresent the rate of recession especially during the transition of a land-terminating to a lake-terminating environment.

Plain Language Summary Lakes form at the margins of glaciers as meltwater accumulates against hillsides and behind ridges of glacier debris. Lakes at a glacier terminus are known to affect its behavior. However, glaciers terminating into such lakes are usually absent from computer simulations, and the effects of these lakes on the rates of deglaciation and on glacier behavior are poorly quantified. In this study, we tested the effect of a lake on glacier recession under two different scenarios; a land-terminating *versus* a lake-terminating glacier. We used an ice flow model called BISICLES and applied it to what was once the Pukaki Glacier in New Zealand during the end of the last ice age. We found that the presence of a lake caused the glacier to recede more than 4 times further and it accelerated ice flow by up to 8 times when compared to the same glacier that terminated on land under the same climate. Our simulated lake processes predominantly influenced the glacier over decades to centuries rather than over millennia. We suggest, therefore, that simulations of glacier evolution ignoring glacial lakes will likely misrepresent the timing and rate of recession, especially during the transition from a land-terminating to a lake-terminating environment.

1. Introduction

Sustained glacier recession is driving the development of proglacial lakes at the termini of glaciers as meltwater accumulates within bedrock basins, behind moraine ridges and outwash fan heads, or is impounded by dead ice (Carrivick & Tweed, 2013). Glaciers in contact with a lake are receding more rapidly than their land-terminating counterparts, for example, in the Himalaya (Maurer et al., 2019; Tsutaki et al., 2019), in Alaska (Larsen et al., 2007; Willis et al., 2012), and in New Zealand (Chinn et al., 2012). Glaciers terminating in proglacial lakes can lose mass by several mechanisms in addition to melt from energy exchanges at the ice surface, namely, calving and subaqueous melting, collectively known as frontal ablation (Maurer et al., 2016; Sakai et al., 2009; Truffer & Motyka, 2016; Watson et al., 2020). Glaciers hosting proglacial lakes can, therefore, be partially decoupled from climatic forcing due to the effects of frontal ablation (King et al., 2018; Kirkbride, 1993), causing nonlinear responses in ice geometry and behavior (Benn et al., 2012).

Recent observations, both field-based (e.g., Watson et al., 2020) and via satellite imagery (e.g., King et al., 2019), have highlighted the spatiotemporal frequency and magnitude of changes in glacial lakes and the associated glaciers that feed meltwater to them. However, field-based measurements are limited to

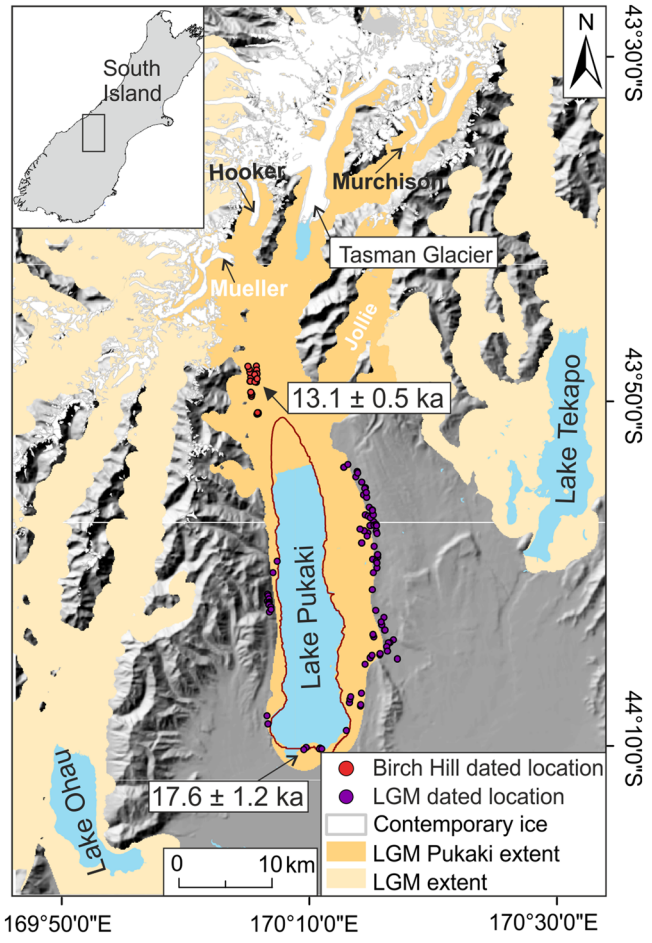

Figure 1. Location and geographical setting of the Pukaki Glacier. Contemporary ice extent (from Global Land Ice Measurements from Space, 2019) overlain on hill-shaded digital elevation model (from Land Information New Zealand, 2019). Dated sample locations for LGM and Birch Hill moraines are mapped as purple and red dots, respectively, and their mean exposure ages are labeled. This figure is also the extent of the model domain. The red contour represents 0 m above lake-level used in LAKE simulations.

individual sites, usually spanning a single ablation season (e.g., Purdie & Fitzharris, 1999), and remote sensing investigations are limited to the last decade or so at most. Nonetheless, in order to have confidence in projections of glacier and ice sheet mass loss, it is critical to quantify changes in glacier and lake extent and behavior over longer timescales. It is imperative to understand if the trajectories of recent rates of mass loss from lake-terminating glaciers (e.g., Dykes et al., 2011; King et al., 2019; Purdie et al., 2016; Quincey & Glasser, 2009) can be extrapolated into the future. A solution to this dearth of process data, and to the restricted timeframe from which it comes, is to assess the impacts of ice-marginal lakes on the evolution of glacial systems as represented in the Quaternary geological record.

The Quaternary geological record contains abundant evidence of the impacts of proglacial lakes on continental ice sheet geometry and behavior, and hence on climate and sea level (Krinner et al., 2004; Li et al., 2012; Stokes & Clark, 2004; Törnqvist et al., 2004). For example, studies of the Laurentide Ice Sheet during the Last Glacial Maximum (LGM) have shown that deglaciation was characterized by complex reorganizations in flow patterns and dynamics which, in part, have been attributed to proglacial lakes triggering and sustaining rapid ice flow (Utting & Atkinson, 2019). Many reconstructions of continental ice sheets during the last glacial cycle using ice flow models (e.g., Gregoire et al., 2016; Stokes et al., 2012) do not include proglacial lakes. A notable exception is the recent work of Hinck et al. (2019) who present an algorithm that efficiently identifies and fills isolated lake basins with the corresponding maximum water level and has been applied to ice sheet reconstructions of North America and the present day. However, with estimated maximum areal extents of several hundred thousand kilometers (e.g., ~710,000 km^2; Glacial Lake Agassiz-Ojibway), ice sheet-lake reconstructions on this continental ice sheet scale are not directly applicable to mountain glaciers in regions such as the Himalaya, Patagonia, or New Zealand.

To date, no studies have isolated the effects of proglacial lakes specifically on glacier dynamics. Glacier sensitivity to the presence of a proglacial lake at its terminus and to the dynamics of that lake remains entirely unknown from the Quaternary record at the sub-ice sheet scale. Consequently, investigations are needed at the glacier scale to understand more about the rate of recession under the controls of proglacial lake development. The aim of this study is, therefore, to quantify the impact of an ice-contact proglacial lake on the geometry (grounding line position, ice margin shape, and ice thickness) and ice flow of a mountain glacier during recession. To achieve this, we used a well-resolved landform record as an empirical foundation for simple scenario modeling experiments.

2. Study Area

During the LGM, glaciers extended out from the Southern Alps icefield in New Zealand to form local piedmont lobes (Barrell et al., 2011; Golledge et al., 2012; James et al., 2019). The largest of which extended into and across the basin now occupied by Lake Pukaki and is referred to as the Pukaki Glacier (e.g., McKinnon et al., 2012; Putnam, Denton, et al., 2010). At its maximum LGM extent the Pukaki Glacier was ~85 km long and covered 1,300 km^2 (Figure 1; Porter, 1975). Early geological and geomorphological work relating to the Pukaki Glacier is summarized by Barrell and Read (2014), but of most significance is that the Pukaki valley contains an exceptionally well-preserved geomorphological record of lateral and terminal moraines (Barrell et al., 2011). The moraines trend north to south and the ridges parallel the eastern shore of Lake Pukaki and have been dated in many geochronological

campaigns (e.g., Doughty et al., 2015; Kelley et al., 2014; Putnam, Denton, et al., 2010; Putnam, Schaefer, et al., 2010; Schaefer et al., 2006, 2015; Strand et al., 2019). Those moraines most relevant to this study are an inner line at the southern end of the lake, with a mean surface exposure dating (SED) age of 17.6 ± 1.2 ka, thus marking a deglacial age after the onset of the LGM termination (Darvill et al., 2016; Figure 1) and the Birch Hill moraines at the northern, up-valley end of the lake which have a mean SED age of 13.1 ± 0.5 ka (Darvill et al., 2016; Figure 1) representing either a still stand or a readvance of the ice margin during the Antarctic Cold Reversal (ACR; Putnam, Denton, et al., 2010). It has been argued that the time gap of ~5,000 years and the large valley distance of >25 km between these sets of moraine clusters is evidence for an abrupt glaciation termination with virtual ice collapse, in tandem with Antarctic warming (Schaefer et al., 2006).

3. Methods

3.1. Model Description and Domain

In this study, we use the vertically integrated ice flow model BISICLES (Cornford et al., 2013). BISICLES was chosen for its efficient and accurate representation of the dynamics of marine grounded ice sheets and for its process-representation permitting ice shelf formation, grounding line migration, and ice surface lowering. BISICLES has previously been applied to simulations of both contemporary (e.g., Antarctica, Cornford et al., 2015; Berger et al., 2016) and paleo ice sheets (e.g., The British-Irish Ice Sheet; Gandy et al., 2018, 2019), as well as to smaller icefields (e.g., Patagonia). The dynamical equations in BISICLES fall into type "L1L2" of hybrid ice sheet modeling approaches (Hindmarsh, 2004), where the longitudinal stresses are treated as depth dependent, and are included in the computation of stresses driving the ice flow (Schoof & Hindmarsh, 2010). This approach includes elements from both the shallow ice approximation and shallow shelf approximation, which is more appropriate for modeling fast flowing and floating ice than either the shallow ice approximation or shallow shelf approximation alone (Bueler & Brown, 2009).

3.2. Experimental Design

We "spin-up" the model to produce a steady state ice geometry representative of the end of the LGM at 18 ka (Figure S2 in the supporting information) as given from field evidence (Barrell et al., 2011) and by other modelled reconstructions (e.g., Golledge et al., 2012; James et al., 2019). Recession of two scenarios were then simulated: a land-terminating Pukaki Glacier ("LAND") and a lake-terminating Pukaki Glacier ("LAKE"). LAND was forced by an idealized climate only, whereas LAKE was forced by the same idealized climate in addition to frontal ablation (subaqueous melting and calving). Our scenario experiments were informed by geochronological data from the moraines at Pukaki but were not best fitted to them due to the lack of evidence of ice margin position in the basin between the LGM and the ACR. The position of the moraines separated by >25 km (Figure 1) enabled Porter (1975) to estimate an equilibrium line altitude (ELA) for the LGM and Birch Hill ice extents of 1,225 and 1,600 m above sea level, respectively. Assuming that the glacier was in steady state at both times, the difference in ELA and the mean exposure ages of the moraines, representing ~5,000 years between formation, enabled us to calculate a linear rate of ELA rise. Climate forcing is therefore specified in our model via a linear increase in ELA of 0.05 m per year, or for clarity 50 m ELA rise per millennium. To capture deglaciation from the end of the LGM to up-valley of the Birch Hill limits, we ran both LAND and LAKE simulations from the spin-up extent (Figure S2) for 10 kyr.

3.3. Boundary Conditions and Parameterization

Specifying an idealized climatic change, initiating the scenarios with an equilibrium ice extent initial condition and keeping all other boundary conditions and parameters identical within both sets of model simulations, enabled us to isolate the internal mechanisms of recession, specifically assessing the relative role of frontal ablation on ice dynamics. Information about the model initial conditions such as bed topography is discussed in Text S1 and Figure S1. Key model parameters are summarized in Table S1. We used a linear viscous sliding law ($m = 1$), which accounted for sliding that did not require basal melt. Our choice of calving and subaqueous melt parameter values in LAKE were informed by our sensitivity testing (Text S4 and Figure S3), which itself was based on values from contemporary observations reported in the literature (Table S2). We ran 10 simulations of LAKE: 5 prescribing a different subaqueous melt rate (0, −1, −10, −50, and −100 m a^{-1}) and 5 prescribing a different calving rate (10, 50, 100, 500, and 1,000 m a^{-1};

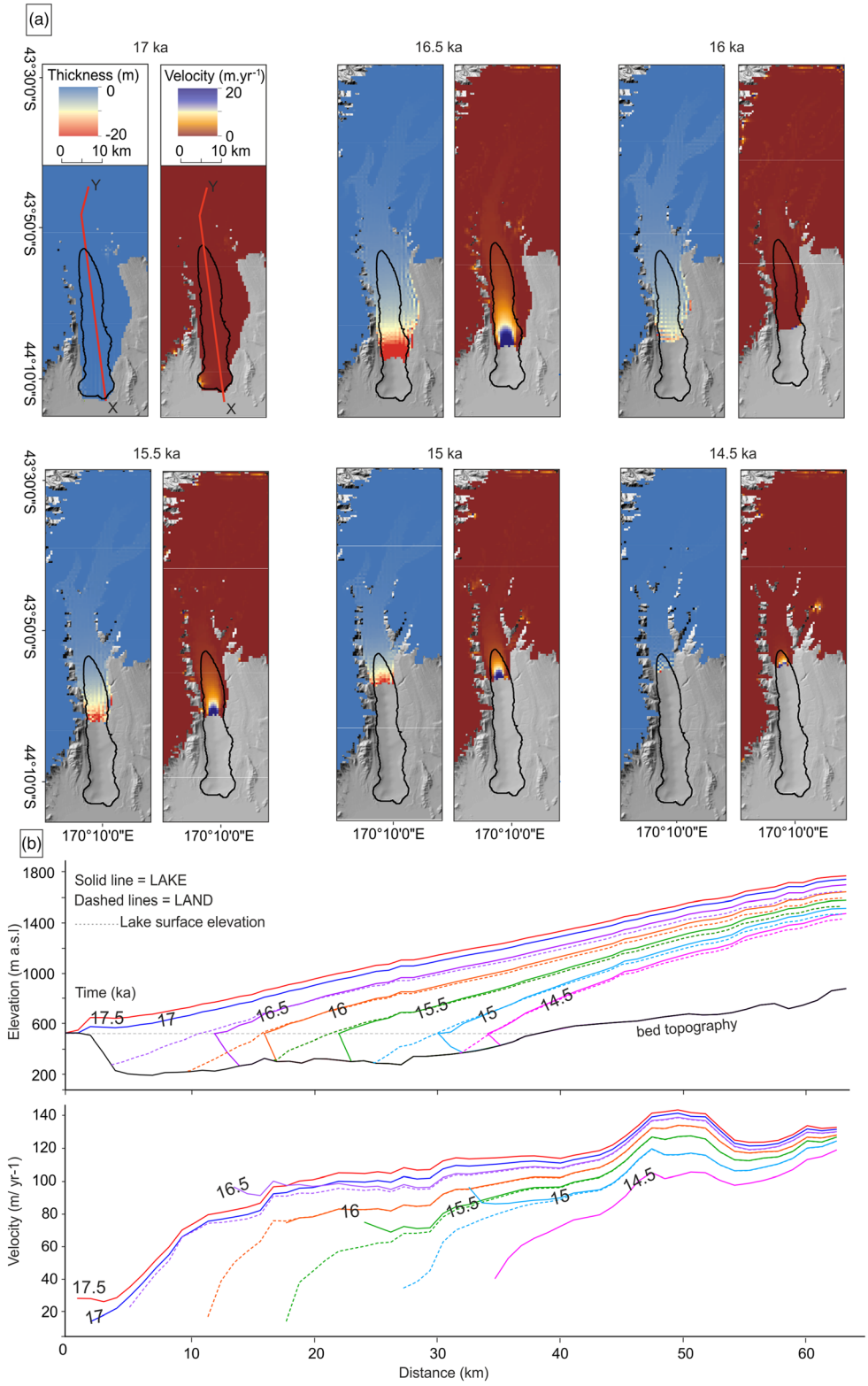

Figure 2. (a) Differences in ice thickness and velocity between LAND and LAKE simulations in which a subaqueous melt of −50 m a^{-1} and a calving rate of 100 m a^{-1} were prescribed. Map scales are capped for clarity at −20 m thickness and 20 m a^{-1} velocity, but differences of up to 242 m and 85 m a^{-1} were simulated, respectively. (b) Ice surface and velocity profiles from *X-Y* transect in panel (a). Dashed lines represent LAND, and solid lines represent LAKE. Time (ka) is labeled on each corresponding line.

Table S3) each time. We report LAKE as the calculated mean output value from these simulations. Our sensitivity testing revealed that subaqueous melt rate had a relatively larger effect on glacier geometry and behavior, but that calving rate did not. The subaqueous melt flux was masked only to floating ice. Calving into the lake was modeled according to a crevasse depth criterion (Benn et al., 2007; Nick et al., 2010). Surface crevasses opened to the depth where tensile stress and water pressure are balanced by ice overburden pressure (Weertman, 1973), and calving took place when the crevasses reached the waterline. Water pressure was set by assuming that crevasses filled with up to 100 m of water. Noting an absence of field data on fluctuating lake level, the lake level was held constant throughout the LAKE simulations.

There are several differences to consider when applying an ice flow model, designed to simulate marine-terminating environments, to lacustrine settings (Text S3). To account for the differences between marine and lake-terminating glacier termini, we made the following specifications: (i) the density of freshwater (1,000 kg m^{-3}; Table S1) was used to compute buoyancy as opposed to the density of saline water; (ii) smaller calving and subaqueous melt rates were used than are usually prescribed within ice sheet models (Tables S2 and S3); and (iii) water temperature was accounted for within the subaqueous melt flux component but held constant because thermal stratification is assumed unimportant on millennial timescales (Carrivick & Tweed, 2013).

4. Results

We computed grounding line recession of the Pukaki Glacier over tens of kilometers and examined the response of glacier geometry (grounding line position, ice margin shape, and ice thickness), ice flow, and rate of recession to the perturbation of terminus environment (LAND versus LAKE). Both simulations caused recession of the Pukaki Glacier terminus from the lip of its overdeepened basin northward past the Birch Hill moraines (Figure 1) within 6 kyrs (Figures S4–S6), thus in broad agreement with the rate of recession interpreted from the glacial geomorphology (e.g., Putnam, Denton, et al., 2010). However, in contrast to the geomorphological record, our simulations suggest the time-transgressive nature of ice margin recession. Substantial differences in grounding line position (terminus position in LAND), ice thickness, and velocity were simulated between LAND and LAKE from 16.5 to 14.5 ka (Figures 2 and 3). We specifically focus on comparing glacier geometry and behavior at the grounding line although the effects of LAKE on ice thickness and velocity were propagated up-glacier (Figure 2).

4.1. Ice Margin Geometry

The Pukaki Glacier in LAND was grounded across its entirety throughout the duration of the simulation (Figures 2b and S4). In LAKE, the glacier was wedge shaped and floating where the grounding line remained ~2 km behind the terminus (Figure 2b). The width of the glacier in LAND was much narrower in comparison to that within LAKE, which spanned the width of the overdeepened basin (Figure S5) as an ice cliff. Throughout recession, the glacier in LAND became narrower (Figure S5), whereas in LAKE it remained at the same width throughout recession. The maximum thickness of the Pukaki Glacier in both model simulations was 1,300 m (at 18 ka), occurring in the trunk of the glacier in the narrowest part of the valley (Figure S2). Ice thickness in LAND was thinner, increasingly so toward the terminus (Figures 2 and 3), and varied between 15 and 74 m. During the first 100 years after the glacier receded into the basin in LAKE, progressively thicker ice floated; the thickness of ice at the grounding line in LAKE increased substantially up to 345 m at 16.9 ka (330 m thicker than LAND; Figure 3) and then steadily declined throughout the rest of the simulation. Lake effects contributed 96% of the total ice thickness after 100 years (at 16.9 ka) and diminished to 48% by the end of the simulations.

4.2. Ice Margin Position

During the first 1,000 years (from 18 to 17 ka), the terminus receded 2 km in both simulations (Figures 2b and 3) but remained grounded on the lip of the overdeepened basin (Figure 2b). This recession was land-terminating and so driven by the rising ELA only. With continued recession, the Pukaki Glacier in the LAKE and LAND scenarios diverged from each other. The maximum divergence occurred from 17 to 16.9 ka at the time of entering the over-deepened basin. The position of the ice margin in the two scenarios then slowly converged again over the next 1,500 years (by 14.5 ka; Figure 3). The rate of recession slowed as the glacier receded through its over-deepened basin (Figures 2b and 3). The difference between simulations in position

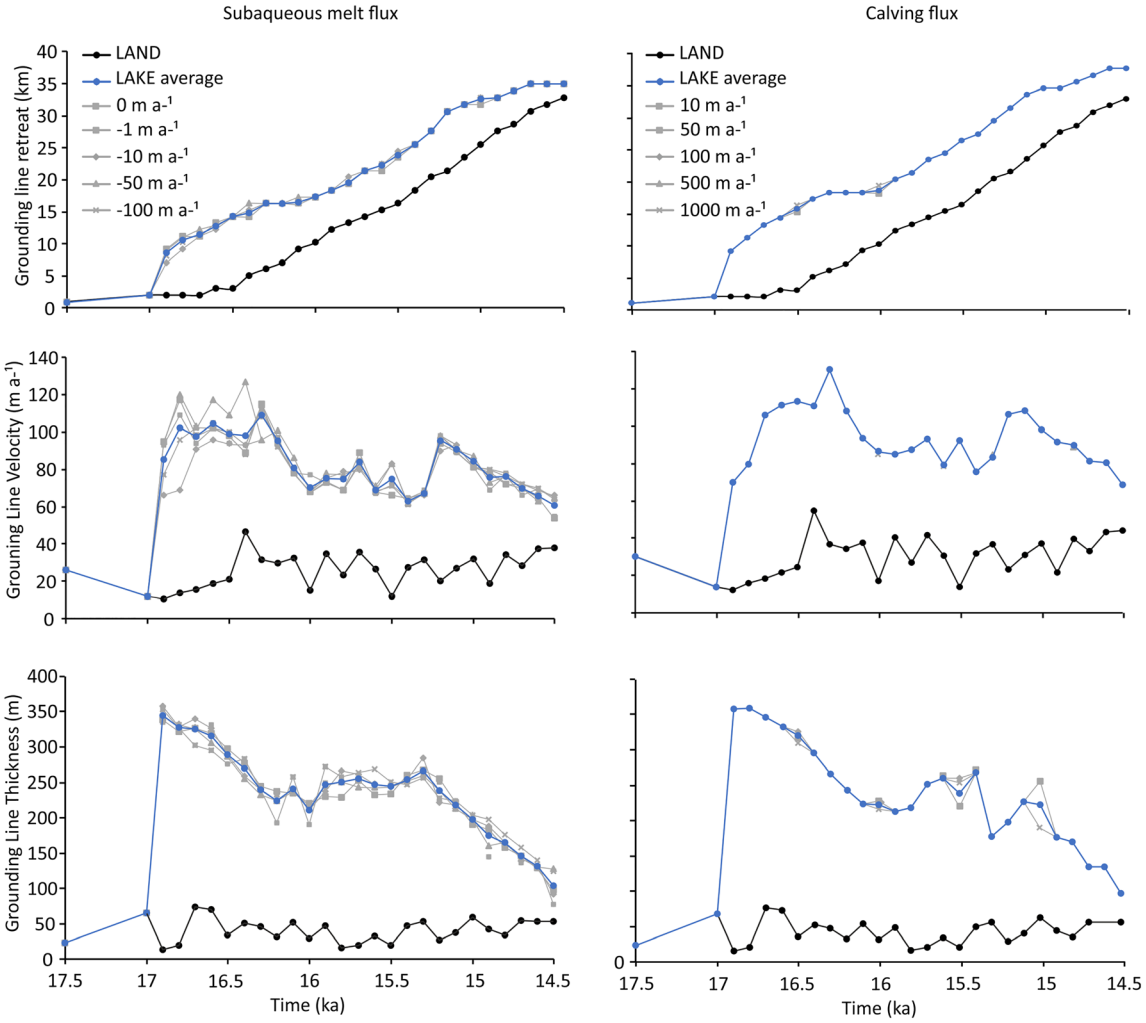

Figure 3. Grounding line position (LAKE) and terminus position (LAND), ice velocity, and ice thickness for LAND and LAKE simulations plotted at 100-year increments from a part of the 10 kyr-long simulations between 17.5 and 14.5 ka. Gray lines represent varied subaqueous melt and calving rates, derived from the literature (Table S3) in LAKE simulations, and the blue line represents the mean of these output values.

of the grounding line in LAKE and the terminus in LAND was greatest at 16.5 ka where the grounding line had receded 14 km by 16.5 ka in LAKE compared to 3 km of terminus recession during the same period in LAND (Figures 2b and 3). At 16.5 ka, the grounding line in LAKE had receded nearly 6 times further than the terminus of LAND. Lake effects contributed 76% of total grounding line recession after 100 years (at 16.9 ka). This increased to 82% of cumulative grounding line recession after 300 years before diminishing to 6% by the end of the simulations.

4.3. Ice Velocity

Maximum ice velocities of 141 m a^{-1} occurred in both simulations at 17.5 ka in the main trunk of the glacier where the ice was thickest (~48 km up-glacier where the valley narrows just north of the confluence of the Jollie valley along the *X*-*Y* transect in Figure 2a). Mean ice velocities at the terminus in both simulations prior to 16.5 ka were between 10 and 20 m a^{-1} when the ice margin was grounded on the lip of the overdeepened basin. The greatest differences in ice velocity between LAND and LAKE were at the terminus (Figure 2). Grounding line velocities in LAKE were amplified above LAND terminus velocities by 1 order of magnitude (Figure 3). Low mean velocities varied in LAND between 11 and 47 m a^{-1}, whereas velocities were relatively increased at the calving ice margin of LAKE (Figure 2b). The lowest velocities in LAKE occurred at the lateral ice margin where the ice was grounded on the valley sides (Figure 2a). Figure 3

displays 700 years of acceleration at the grounding line in LAKE, showing steadily increasing grounding line velocities until reaching a peak of 109 m a^{-1} at 16.3 ka. The biggest difference in velocity between the LAND terminus and the grounding line of LAKE was 88 m a^{-1}, which occurred at 16.8 ka. Lake effects contributed 87% of the total ice velocity after 100 years (at 16.9 ka) and diminished to 37% by the end of the simulations.

5. Discussion

Our numerical modeling illustrates and explains the substantial effects that a lake at the terminus of a glacier can have on the geometry (grounding line position, ice margin shape, and ice thickness), ice flow, and rate of recession when compared to the same glacier terminating on land and under the same climate. These effects can be summarized as being more rapid ice margin recession, ice surface drawdown, and ice velocity acceleration (Figures 2b and 3), and in that regard they confirm prevailing conceptual models (e.g., Carrivick & Tweed, 2013). However, in this study we have quantified the spatiotemporal nature of these effects, and we are able to shed light on the driving mechanisms responsible for these differences.

5.1. Glacier Geometry and Behavior

Differences in glacier geometry and behavior between the simulations became more marked as the lake-terminating glacier encountered progressively deeper water within its overdeepened basin and frontal ablation became proportionally more effective (Figure 2). The divergence between the two simulations, that is, the effect of the proglacial lake, diminished once the glacier terminus was receding up a normal-grade bed slope (Figures 2b and 3). The initial rapid recession indicates that the lake-terminating glacier was abruptly forced out of equilibrium with the prescribed climate warming. Once the effect of the lake was no longer pronounced, the glacier entered a period of adjustment to re-equilibrate with the prescribed warming.

The land-terminating scenario displayed a linear rate of recession after 16.5 ka, whereas the lake-terminating scenario displayed an initial acceleration of recession by 16.9 ka with a near-constant rate of recession thereafter (Figure 3). After their initial differences, the rates of recession between the two scenarios were similar. We identify a "period of collapse" in the lake-terminating scenario from 17 to 16.5 ka. The timing of collapse was simulated to occur when the ice margin receded from the lip of its overdeepened basin, down a reverse-grade bed slope, and into deep water (>200 m; Figures 2b and S1). The early amplified recession during this period is explained by recession of the grounding line into its ice-contact proglacial lake that was both expanding laterally and deepening as the glacier receded northward into its basin (Figure 3). The reverse gradient of the bed slope persists for ~4 km (Figures 2b and S1) of recession. This, and the transition of the terminus to a position of a shallowing and then of a normally graded bed slope (Figure 2b), explains why the effect of amplified recession does not increase through time.

We observe that the faster recession of the Pukaki Glacier before 16.5 ka in LAKE is related, at least in the model, to a phenomenon known in tidewater glaciers and marine ice sheets as marine ice sheet instability (Katz & Worster, 2010; Schoof, 2007; Thomas & Bentley, 1978; Weertman, 1974). All else being equal, recession of the grounding line along a reverse-grade slope (deepening toward the center of the glacier) results in faster flow and further recession. This effect can potentially be countered by buttressing (Gudmundsson, 2013) or spatially variable friction (Brondex et al., 2017). However, both are unlikely conditions in ice-marginal lakes. We propose that the processes and feedbacks involved in marine ice sheet instability extend beyond the marine realm to glaciers that terminate in water in large overdeepened basins. Indeed, Larsen et al. (2015) suggested that the presence of large proglacial lakes that occupy substantial overdeepenings may lead to an ice margin geometry that is more akin to tidewater glaciers; thus, similar feedbacks may operate to induce ice front recession and ice loss. The duration and magnitude of ice loss from lake-terminating glaciers will therefore depend on (i) the size of each glacial overdeepening, with glaciers only reaching equilibrium once the terminus can recede to an altitude above the lake they host, and (ii) ice thickness because that determines the threshold for flotation.

5.2. Wider Implications

The timing of recession of the Pukaki Glacier is thought to be consistent with the onset of temperature and atmospheric CO_2 increases indicated by Antarctic ice cores (Schaefer et al., 2006). However, we propose that this atmospheric warming likely only initiated glacier recession from its LGM position, which forced the terminus into its overdeepened basin and eventually into deep lake water. After which, our modeling suggests

that both frontal ablation processes and climatic warming contributed to local glacier collapse. Once the Pukaki Glacier became lake terminating, its terminus recession was likely partially decoupled from climate. Such hypotheses have been previously proposed in New Zealand for other glaciers (e.g., Shulmeister et al., 2019; Sutherland, Carrivick, Evans, et al., 2019; Sutherland, Carrivick, Shulmeister, et al., 2019) and have been confirmed for glaciers elsewhere by empirical data, for example, from Patagonia (Bendle et al., 2019). This partial decoupling of glacier behavior from climate is potentially important for interpreting the evolution of New Zealand mountain glaciers, particularly over decadal timescales.

The large changes observed from the fine temporal resolution (100 years) in our model (Figure 3) reveals variability between the LAND and LAKE scenarios on decadal to centennial scales but not over millennia. The rapid acceleration in recession followed by a near-constant rate of recession, and the behavior captured within our lake-terminating simulation has marked similarities with observations from contemporary glaciers. Rapid changes to lake-terminating glaciers have been shown to occur over two to three decades in the central Himalaya (Basnett et al., 2013; King et al., 2019; Song et al., 2017). King et al. (2018) specifically showed that Himalayan glaciers can undergo periods of ice acceleration and enhanced mass loss with the onset and continuation of lake formation, followed by ice deceleration and mass loss stabilization as the glacier recedes out of the overdeepening. Based on this empirical evidence and our numerical modeling, we suggest that this spatiotemporal pattern is common and virtually all lake-glacier interactions will evolve in this way, where the magnitude of a lake effect and the time duration of those effects are proportional to the size/depth and elongation of the lake basin, as well as to individual ice geometries and ice dynamics.

The persistence of proglacial lake effects upon ice dynamics requires more detailed study. Specifically, decadal- to centennial-scale projections will require ice sheet and mountain glacier modeling that incorporate proglacial lake evolution. With lake-terminating glaciers becoming more numerous and larger (e.g., Carrivick & Quincey, 2014), the likely increasing influence of frontal ablation processes must be incorporated into ice dynamics models with account for fluctuating lake levels driven by contributions to the meltwater flux. Future work should also consider the importance of several other mechanisms that could further enhance recession of a lake-terminating glacier in comparison to a land-terminating glacier, such as convective warming of the ice by thermal warming of lake water, and wind-driven wave erosion (Mallalieu et al., 2020).

6. Conclusions

This study has (i) assessed the timescale over which the impact of lake processes influence mountain glacier dynamics and (ii) quantified the importance of lake processes relative to climatic forcing. We have shown that a glacier terminus in contact with a lake receded a maximum of more than 4 times further and by up to 8 times faster than a land-terminating ice margin under the same climate warming. This acceleration was short-lived, however, relative to the overall timescale of our simulations, and these maximum lake effects occurred for <10% of the simulation when the lake initially made contact with the ice margin. After which, the two scenarios followed similar trajectories. Our results suggest that 82% of cumulative grounding line recession, 87% of total velocity, and 96% of total ice thickness can be attributed to lake effects. These are maximum values, and they occur during the early stages of recession (within a few hundred years) as the ice margin recedes down a retrograde slope, before diminishing in effect to 6% of grounding line recession, 37% of total velocity, and 48% of total ice thickness by the end of the simulations. We attribute the divergence in behavior of the lake-terminating scenario, relative to the land-terminating scenario, to the combination of a reverse-grade bed slope and frontal ablation resulting in increased ice flow rates at the grounding line and driving stress as the control. When meltwater is impounded within the overdeepened basin, the glacier can (i) float, thereby permitting basal melt, and (ii) calve, thereby permitting mechanical mass loss. Both mechanisms act independent of climate-driven surface melting and produce accelerated ice flow causing compression of the glacier tongue thus steepening the ice surface slope and increasing longitudinal driving stress. The glacier progressively thins and accelerates until the bed slope becomes normally graded, and the ice surface slope matches the bed slope. Although these processes have been conceptualized, our study has added spatiotemporal quantification.

Climate warming is important in order to initiate glacier recession and the development of an ice-contact proglacial lake. However our numerical modeling highlights the transition from a land-terminating to a lake-terminating environment can dramatically perturb glacier geometry and behavior. This partial decoupling from climatic forcing is particularly important over decadal to centennial timescales. We contend that ice sheet outlets or mountain glaciers that develop ice-marginal lakes will experience accelerated mass loss, where the absolute spatiotemporal magnitude of that mass loss relates to the depth and elongation of the associated overdeepening, the lake water depth, and glacier characteristics such as ice thickness and velocity.

Data Availability Statement

The digital elevation model used is available from Land Information New Zealand (2019); the LGM bed elevation is available from McKinnon et al. (2012) and James et al. (2019). The glacier outlines are available from Global Land Ice Measurements from Space (2019).

Acknowledgments

J. L. S. and N. G. were funded by PhD studentships from the Natural Environment Research Council (NERC) SPHERES Doctoral Training Partnership (NE/L002574/1). N. G. was also supported by the UKRI Future Leaders Fellowship Project MR/S016961/1. J. L. S. acknowledges funding from The Brian Mason Scientific and Technical Trust. This work was undertaken on ARC3, which is part of the High-Performance Computing facilities at the University of Leeds, UK. J. L. S. thanks Richard Rigby for help in installing BISICLES and for his continuous and excellent IT support. William James is thanked for the New Zealand LGM ice extent and bed topography. Trevor Chinn is thanked for insightful discussions on glacier-lake interactions. This study did not use any new data. We thank Ann Rowan and two anonymous reviewers for constructive comments that improved the manuscript.

References

Barrell, D. J. A., Andersen, B. G., Denton, G. H., & Smith-Lyttle, B. (2011). Glacial Geomorphology of the Central South Island, New Zealand. *GNS Science Monograph*, *27*.

Barrell, D. J., & Read, S. A. (2014). The deglaciation of Lake Pukaki, South Island, New Zealand—A review. *New Zealand Journal of Geology and Geophysics*, *57*, 86–101. https://doi.org/10.1080/00288306.2013.847469

Basnett, S., Kulkarni, A., & Bolch, T. (2013). The influence of debris cover and glacial lakes on the recession of glaciers in Sikkim Himalaya, India. *Journal of Glaciology*, *59*, 1035–1046. https://doi.org/10.3189/2013JoG12J184

Bendle, J. M., Palmer, A. P., Thorndycraft, V. R., & Matthews, I. P. (2019). Phased Patagonian Ice Sheet response to Southern Hemisphere atmospheric and oceanic warming between 18 and 17 ka. *Scientific Reports*, *9*(1), 1–9. https://doi.org/10.1038/s41598-019-39750-w

Benn, D. I., Bolch, T., Hands, K., Gulley, J., Luckman, A., Nicholson, L. I., et al. (2012). Response of debris-covered glaciers in the Mount Everest region to recent warming, and implications for outburst flood hazards. *Earth-Science Reviews*, *114*(1–2), 156–174. https://doi.org/10.1016/j.earscirev.2012.03.008

Benn, D. I., Warren, C. R., & Mottram, R. H. (2007). Calving processes and the dynamics of calving glaciers. *Earth-Science Reviews*, *82*(3–4), 143–179. https://doi.org/10.1016/j.earscirev.2007.02.002

Berger, S., Favier, L., Drews, R., Derwael, J. J., & Pattyn, F. (2016). The control of an uncharted pinning point on the flow of an Antarctic ice shelf. *Journal of Glaciology*, *62*(231), 37–45. https://doi.org/10.1017/jog.2016.7

Brondex, J., Gagliardini, O., Gillet-Chaulet, F., & Durand, G. (2017). Sensitivity of grounding line dynamics to the choice of the friction law. *Journal of Glaciology*, *63*(241), 854–866. https://doi.org/10.1017/jog.2017.51

Bueler, E., & Brown, J. (2009). Shallow shelf approximation as a "sliding law" in a thermomechanically coupled ice sheet model. *Journal of Geophysical Research*, *114*, F03008. https://doi.org/10.1029/2008jf001179

Carrivick, J. L., & Quincey, D. J. (2014). Progressive increase in number and volume of ice-marginal lakes on the western margin of the Greenland Ice Sheet. *Global and Planetary Change*, *116*, 156–163. https://doi.org/10.1016/j.gloplacha.2014.02.009

Carrivick, J. L., & Tweed, F. S. (2013). Proglacial lakes: Character, behaviour and geological importance. *Quaternary Science Reviews*, *78*, 34–52. https://doi.org/10.1016/j.quascirev.2013.07.028

Chinn, T., Fitzharris, B. B., Willsman, A., & Salinger, M. J. (2012). Annual ice volume changes 1976–2008 for the New Zealand Southern Alps. *Global and Planetary Change*, *92*, 105–118. https://doi.org/10.1016/j.gloplacha.2012.04.002

Cornford, S. L., Martin, D. F., Graves, D. T., Ranken, D. F., Le Brocq, A. M., Gladstone, R. M., et al. (2013). Adaptive mesh, finite volume modeling of marine ice sheets. *Journal of Computational Physics*, *232*, 529–549. https://doi.org/10.1016/j.jcp.2012.08.037

Cornford, S. L., Martin, D. F., Payne, A. J., Ng, E. G., Le Brocq, A. M., Gladstone, R. M., et al. (2015). Century-scale simulations of the response of the West Antarctic Ice Sheet to a warming climate. *The Cryosphere*, *9*, 1579–1600. https://doi.org/10.5194/tc-9-1579-2015

Darvill, C. M., Bentley, M. J., Stokes, C. R., & Shulmeister, J. (2016). The timing and cause of glacial advances in the southern mid-latitudes during the last glacial cycle based on a synthesis of exposure ages from Patagonia and New Zealand. *Quaternary Science Reviews*, *149*, 200–214. https://doi.org/10.1016/j.quascirev.2016.07.024

Doughty, A. M., Schaefer, J. M., Putnam, A. E., Denton, G. H., Kaplan, M. R., Barrell, D. J., et al. (2015). Mismatch of glacier extent and summer insolation in Southern Hemisphere mid-latitudes. *Geology*, *43*, 407–410. https://doi.org/10.1130/G36477.1

Dykes, R. C., Brook, M. S., Robertson, C. M., & Fuller, I. C. (2011). Twenty-first century calving retreat of Tasman Glacier, Southern Alps, New Zealand. *Arctic, Antarctic, and Alpine Research*, *43*(1), 1–10. https://doi.org/10.1657/1938-4246-43.1.1

Gandy, N., Gregoire, L. J., Ely, J., Clark, C., Hodgson, D. M., Lee, V., et al. (2018). Marine ice sheet instability and ice shelf buttressing of the Minch Ice Stream, northwest Scotland. *The Cryosphere*, *12*, 3635–3651. https://doi.org/10.5194/tc-12-3635-2018

Gandy, N., Gregoire, L. J., Ely, J. C., Cornford, S. L., Clark, C. D., & Hodgson, D. M. (2019). Exploring the ingredients required to successfully model the placement, generation, and evolution of ice streams in the British-Irish Ice Sheet. *Quaternary Science Reviews*, *223*, 105915. https://doi.org/10.1016/j.quascirev.2019.105915

Global Land Ice Measurements from Space (2019). Randolph glacier inventory, https://www.glims.org/RGI/index.html last visited March, 2020

Golledge, N. R., Mackintosh, A. N., Anderson, B. M., Buckley, K. M., Doughty, A. M., Barrell, D. J., et al. (2012). Last Glacial Maximum climate in New Zealand inferred from a modelled Southern Alps icefield. *Quaternary Science Reviews*, *46*, 30–45. https://doi.org/10.1016/j.quascirev.2012.05.004

Gregoire, L. J., Otto-Bliesner, B., Valdes, P. J., & Ivanovic, R. (2016). Abrupt Bølling warming and ice saddle collapse contributions to the Meltwater Pulse 1a rapid sea level rise. *Geophysical Research Letters*, *43*, 9130–9137. https://doi.org/10.1002/2016GL070356

Gudmundsson, G. H. (2013). Ice-shelf buttressing and the stability of marine ice sheets. *The Cryosphere*, *7*(2), 647–655. https://doi.org/10.5194/tc-7-647-2013

Hinck, S., Gowan, E. J., & Lohmann, G. (2019). LakeCC: A tool for efficiently identifying lake basins with application to palaeogeographic reconstructions of North America. *Journal of Quaternary Science*, *35*, 422–432. https://doi.org/10.1002/jqs.3182

Hindmarsh, R. C. A. (2004). A numerical comparison of approximations to the Stokes equations used in ice sheet and glacier modeling. *Journal of Geophysical Research*, *109*(F1). https://doi.org/10.1029/2003jf000065

James, W. H., Carrivick, J. L., Quincey, D. J., & Glasser, N. F. (2019). A geomorphology based reconstruction of ice volume distribution at the Last Glacial Maximum across the Southern Alps of New Zealand. *Quaternary Science Reviews*, *219*, 20–35. https://doi.org/10.1016/j.quascirev.2019.06.035

Katz, R. F., & Worster, M. G. (2010). Stability of ice-sheet grounding lines. *Proceedings of the Royal Society A: Mathematical, Physical and Engineering Sciences*, *466*(2118), 1597–1620. https://doi.org/10.1098/rspa.2009.0434

Kelley, S. E., Kaplan, M. R., Schaefer, J. M., Andersen, B. G., Barrell, D. J., Putnam, A. E., et al. (2014). High-precision ^{10}Be chronology of moraines in the Southern Alps indicates synchronous cooling in Antarctica and New Zealand 42,000 years ago. *Earth and Planetary Science Letters*, *405*, 194–206. https://doi.org/10.1016/j.epsl.2014.07.031

King, O., Bhattacharya, A., Bhambri, R., & Bolch, T. (2019). Glacial lakes exacerbate Himalayan glacier mass loss. *Scientific Reports*, *9*, 1–9. https://doi.org/10.1038/s41598-019-53733-x

King, O., Dehecq, A., Quincey, D., & Carrivick, J. (2018). Contrasting geometric and dynamic evolution of lake and land-terminating glaciers in the central Himalaya. *Global and Planetary Change*, *167*, 46–60. https://doi.org/10.1016/j.gloplacha.2018.05.006

Kirkbride, M. P. (1993). The temporal significance of transitions from melting to calving termini at glaciers in the central Southern Alps of New Zealand. *The Holocene*, *3*(3), 232–240. https://doi.org/10.1177/095968369300300305

Krinner, G., Mangerud, J., Jakobsson, M., Crucifix, M., Ritz, C., & Svendsen, J. I. (2004). Enhanced ice sheet growth in Eurasia owing to adjacent ice-dammed lakes. *Nature*, *427*(6973), 429–432. https://doi.org/10.1038/nature02233

LINZ (2019). NZ 8m digital elevation model (2012), https://data.linz.govt.nz/layer/51768-nz-8m-digital-elevation-model-2012/ last visited September 2019

Larsen, C. F., Burgess, E., Arendt, A. A., O'neel, S., Johnson, A. J., & Kienholz, C. (2015). Surface melt dominates Alaska glacier mass balance. *Geophysical Research Letters*, *42*, 5902–5908. https://doi.org/10.1002/2015GL064349

Larsen, C. F., Motyka, R. J., Arendt, A. A., Echelmeyer, K. A., & Geissler, P. E. (2007). Glacier changes in southeast Alaska and northwest British Columbia and contribution to sea level rise. *Journal of Geophysical Research*, *112*, F01007. https://doi.org/10.1029/2006jf000586

Li, Y. X., Törnqvist, T. E., Nevitt, J. M., & Kohl, B. (2012). Synchronizing a sea-level jump, final Lake Agassiz drainage, and abrupt cooling 8200 years ago. *Earth and Planetary Science Letters*, *315*, 41–50.

Mallalieu, J., Carrivick, J. L., Quincey, D. J., & Smith, M. W. (2020). Calving seasonality associated with melt-undercutting and lake ice cover. *Geophysical Research Letters*, 47, e2019GL086561. https://doi.org/10.1029/2019gl086561

Maurer, J. M., Rupper, S. B., & Schaefer, J. M. (2016). Quantifying ice loss in the eastern Himalayas since 1974 using declassified spy satellite imagery. *The Cryosphere*, *10*(5), 2203–2215. https://doi.org/10.5194/tc-10-2203-2016

Maurer, J. M., Schaefer, J. M., Rupper, S., & Corley, A. (2019). Acceleration of ice loss across the Himalayas over the past 40 years. *Science Advances*, *5*(6), eaav7266. https://doi.org/10.1126/sciadv.aav7266

McKinnon, K. A., Mackintosh, A. N., Anderson, B. M., & Barrell, D. J. (2012). The influence of sub-glacial bed evolution on ice extent: A model-based evaluation of the Last Glacial Maximum Pukaki glacier, New Zealand. *Quaternary Science Reviews*, *57*, 46–57. https://doi.org/10.1016/j.quascirev.2012.10.002

Nick, F., Van der Veen, C. J., Vieli, A., & Benn, D. (2010). A physically based calving model applied to marine outlet glaciers and implications for the glacier dynamics. *Journal of Glaciology*, *56*(199), 781–794. https://doi.org/10.3189/002214310794457344

Porter, S. C. (1975). Equilibrium-line altitudes of late Quaternary glaciers in the Southern Alps, New Zealand. *Quaternary Research*, *5*(1), 27–47. https://doi.org/10.1016/0033-5894(75)90047-2

Purdie, H., Bealing, P., Tidey, E., Gomez, C., & Harrison, J. (2016). Bathymetric evolution of Tasman Glacier terminal lake, New Zealand, as determined by remote surveying techniques. *Global and Planetary Change*, *147*, 1–11. https://doi.org/10.1016/j.gloplacha.2016.10.010

Purdie, J., & Fitzharris, B. (1999). Processes and rates of ice loss at the terminus of Tasman Glacier, New Zealand. *Global and Planetary Change*, *22*(1–4), 79–91. https://doi.org/10.1016/S0921-8181(99)00027-2

Putnam, A. E., Denton, G. H., Schaefer, J. M., Barrell, D. J., Andersen, B. G., Finkel, R. C., et al. (2010). Glacier advance in southern middle-latitudes during the Antarctic Cold Reversal. *Nature Geoscience*, *3*(10), 700–704. https://doi.org/10.1038/ngeo962

Putnam, A. E., Schaefer, J. M., Barrell, D. J. A., Vandergoes, M., Denton, G. H., Kaplan, M. R., et al. (2010). In situ cosmogenic 10Be production-rate calibration from the Southern Alps, New Zealand. *Quaternary Geochronology*, *5*(4), 392–409. https://doi.org/10.1016/j.quageo.2009.12.001

Quincey, D. J., & Glasser, N. F. (2009). Morphological and ice-dynamical changes on the Tasman Glacier, New Zealand, 1990–2007. *Global and Planetary Change*, *68*(3), 185–197. https://doi.org/10.1016/j.gloplacha.2009.05.003

Sakai, A., Nishimura, K., Kadota, T., & Takeuchi, N. (2009). Onset of calving at supraglacial lakes on debris-covered glaciers of the Nepal Himalaya. *Journal of Glaciology*, *55*(193), 909–917. https://doi.org/10.3189/002214309790152555

Schaefer, J. M., Denton, G. H., Barrell, D. J., Ivy-Ochs, S., Kubik, P. W., Andersen, B. G., et al. (2006). Near-synchronous interhemispheric termination of the last glacial maximum in mid-latitudes. *Science*, *312*(5779), 1510–1513. https://doi.org/10.1126/science.1122872

Schaefer, J. M., Putnam, A. E., Denton, G. H., Kaplan, M. R., Birkel, S., Doughty, A. M., et al. (2015). The southern glacial maximum 65,000 years ago and its unfinished termination. *Quaternary Science Reviews*, *114*, 52–60. https://doi.org/10.1016/j.quascirev.2015.02.009

Schoof, C. (2007). Ice sheet grounding line dynamics: Steady states, stability, and hysteresis. *Journal of Geophysical Research*, *112*, F03S28. https://doi.org/10.1029/2006jf000664

Schoof, C., & Hindmarsh, R. C. (2010). Thin-film flows with wall slip: An asymptotic analysis of higher order glacier flow models. *Quarterly Journal of Mechanics and Applied Mathematics*, *63*(1), 73–114. https://doi.org/10.1093/qjmam/hbp025

Shulmeister, J., Thackray, G. D., Rittenour, T. M., Fink, D., & Patton, N. R. (2019). The timing and nature of the last glacial cycle in New Zealand. *Quaternary Science Reviews*, *206*, 1–20. https://doi.org/10.1016/j.quascirev.2018.12.020

Song, C., Sheng, Y., Wang, J., Ke, L., Madson, A., & Nie, Y. (2017). Heterogeneous glacial lake changes and links of lake expansions to the rapid thinning of adjacent glacier termini in the Himalayas. *Geomorphology*, *280*, 30–38. https://doi.org/10.1016/j.geomorph.2016.12.002

Stokes, C. R., & Clark, C. D. (2004). Evolution of late glacial ice-marginal lakes on the northwestern Canadian shield and their influence on the location of the Dubawnt Lake palaeo-ice stream. *Palaeogeography, Palaeoclimatology, Palaeoecology*, *215*, 155–171. https://doi.org/10.1016/S0031-0182(04)00467-5

Stokes, C. R., Tarasov, L., & Dyke, A. S. (2012). Dynamics of the North American Ice Sheet Complex during its inception and build-up to the Last Glacial Maximum. *Quaternary Science Reviews*, *50*, 86–104. https://doi.org/10.1016/j.quascirev.2012.07.009

Strand, P. D., Schaefer, J. M., Putnam, A. E., Denton, G. H., Barrell, D. J., Koffman, T. N., & Schwartz, R. (2019). Millennial-scale pulsebeat of glaciation in the Southern Alps of New Zealand. *Quaternary Science Reviews*, *220*, 165–177. https://doi.org/10.1016/j.quascirev.2019.07.022

Sutherland, J. L., Carrivick, J. L., Evans, D. J., Shulmeister, J., & Quincey, D. J. (2019). The Tekapo Glacier, New Zealand, during the Last Glacial Maximum: An active temperate glacier influenced by intermittent surge activity. *Geomorphology*, *343*, 183–210. https://doi.org/10.1016/j.geomorph.2019.07.008

Sutherland, J. L., Carrivick, J. L., Shulmeister, J., Quincey, D. J., & James, W. H. (2019). Ice-contact proglacial lakes associated with the Last Glacial Maximum across the Southern Alps, New Zealand. *Quaternary Science Reviews*, *213*, 67–92. https://doi.org/10.1016/j.quascirev.2019.03.035

Thomas, R. H., & Bentley, C. R. (1978). A model for Holocene retreat of the West Antarctic ice sheet. *Quaternary Research*, *10*(2), 150–170. https://doi.org/10.1016/0033-5894(78)90098-4

Törnqvist, T. E., Bick, S. J., González, J. L., van der Borg, K., & de Jong, A. F. (2004). Tracking the sea-level signature of the 8.2 ka cooling event: New constraints from the Mississippi Delta. *Geophysical Research Letters*, *31*, L23309. https://doi.org/10.1029/2004gl021429

Truffer, M., & Motyka, R. J. (2016). Where glaciers meet water: Subaqueous melt and its relevance to glaciers in various settings. *Reviews of Geophysics*, *54*, 220–239. https://doi.org/10.1002/2015RG000494

Tsutaki, S., Fujita, K., Nuimura, T., Sakai, A., Sugiyama, S., Komori, J., & Tshering, P. (2019). Contrasting thinning patterns between lake- and land-terminating glaciers in the Bhutanese Himalaya. *The Cryosphere*, *13*, 2733–2750. https://doi.org/10.5194/tc-13-2733-2019

Utting, D. J., & Atkinson, N. (2019). Proglacial lakes and the retreat pattern of the southwest Laurentide Ice Sheet across Alberta, Canada. *Quaternary Science Reviews*, *225*, 106034. https://doi.org/10.1016/j.quascirev.2019.106034

Watson, C. S., Kargel, J. S., Shugar, D. H., Haritashya, U. K., Schiassi, E., & Furfaro, R. (2020). Mass loss from calving in Himalayan proglacial lakes. *Frontiers in Earth Science*, *7*. https://doi.org/10.3389/feart.2019.00342

Weertman, J. (1973). Can a water-filled crevasse reach the bottom surface of a glacier. *IASH*, *95*, 139–145.

Weertman, J. (1974). Stability of the junction of an ice sheet and an ice shelf. *Journal of Glaciology*, *13*(67), 3–11. https://doi.org/10.1017/S0022143000023327

Willis, M. J., Melkonian, A. K., Pritchard, M. E., & Ramage, J. M. (2012). Ice loss rates at the Northern Patagonian Icefield derived using a decade of satellite remote sensing. *Remote Sensing of Environment*, *117*, 184–198. https://doi.org/10.1016/j.rse.2011.09.017